# Far-Wing Lineshapes of $CO_2$ and Greenhouse Warming

William Happer
*Department of Physics, Princeton University, Princeton, New Jersey 08544, USA*
(Dated: June 5, 2015)

Using incorrect far-wing lineshapes in computer models can lead to overestimates of the radiative forcing from additional atmospheric $CO_2$ by several tens of per cent. Most of the uncertainty could be eliminated by using modern instrumentation, with high spectral resolution, to determine lineshapes that fit observations at the high-frequency edge of the 667 $cm^{-1}$ band of $CO_2$.

PACS numbers: 33.20.Ea, 33.70.JG, 34.50.Ez, 92.70.Cp

As documented by Fyfe et al.[1], the observed warming of the earth's surface over the past two decades has been much less than predicted by models. The discrepancy is so large, several hundred percent, that it is probably not due to any single flaw in the models but to a number of factors. Here we discuss a factor not mentioned by Fyfe et al.[1]: the feeedback-free, radiative forcing from increasing $CO_2$ may be several tens of percent too large in some models. This is because the individual $CO_2$ absorption lines are not Voigt profiles (Doppler-broadened Lorentzians) but have their far wings suppressed by pedestals.

For a molecule with negligible Doppler shift, making a transition from an upper level $u$ to a lower level $l$, the fraction of radiated energy in the spatial-frequency interval from $\nu$ to $\nu + d\nu$ is $G_{ul}(\nu)d\nu$, where the lineshape function,

$$G_{ul}(\nu) \approx \left(\frac{\mu_{ul}}{\pi\nu_{ul}^4}\right) \frac{\nu^4 \chi_{ul}(\nu)}{\mu_{ul}^2 + (\nu - \nu_{ul})^2}, \qquad (1)$$

is the product of a Lorentzian line core and a multiplicative pedestal function $\chi_{ul}(\nu)$, which determines the far-wing frequencies, generated during the few-picosecond durations of collisions. The Bohr frequency is $\nu_{ul} = (E_u - E_l)/(hc)$, where $E_u$ and $E_l$ are the energies of the upper and lower levels, $h$ is Planck's constant and $c$ is the speed of light. Core linewidth parameters are measured to be $\mu_{ul} \approx 0.1\,p$ $cm^{-1}$ $atm^{-1}$, where $p$ is the air pressure [2]. In the upper stratosphere, where $\mu_{ul} \leq 10^{-4}$ $cm^{-1}$ and comparable to the Doppler broadening, the Lorentzian line core of (1), must be replaced by a Voigt profile, as discussed in the book by Hartmann, Boulet and Robert [3] where one can also find a thorough discussion far-wing lineshapes. Lorentz or Voigt line profiles have $\chi_{ul} = 1$ and correspond to instantaneous collisions.

There have been credible attempts to determine far-wing lineshapes from first-principles calculations, for example, those of Ma *et al.*[4]. However, the collisional interactions required for these calculations are not known with much accuracy, and the far-wing lineshapes really need to be determined experimentally, just as linestrengths, core line-broadening coefficients and other parameters for radiation-transfer calculations have been [2].

To quantify further discussions, we will use the placeholder pedestal

$$\chi_{ul}(\nu) = \ \mathrm{sech}^2([\nu - \nu_{ul}]/\Delta\nu_c), \qquad (2)$$

where $\Delta\nu_c$ is the width. Measurements on bands of $CO_2$, for example by Edwards and Strow [5], suggest that the far wings decrease approximately exponentially with detuning, $|\nu - \nu_{ul}|$, as do the wings of the pedestal (2). But experiments may show that one can choose better model pedestals.

Fig. 1 shows modelled increments $\Delta Z$ in downwelling, spectrally-integrated brightness from the cloud-free zenith for doubling $CO_2$ concentrations $C$ from the present value $C_0 = 400$ ppm. The downwelling "sensitivity," $d\Delta Z/d\log_2 C$ is about 40% larger for pure Voigt lineshapes than for lines with the pedestal (2) and a physically plausible width of $\Delta\nu_c = 2$ $cm^{-1}$. Also shown is the Arrhenius logarithmic approximation [6].

$$\Delta Z = Z_2 \log_2(C/C_0). \qquad (3)$$

We have been unable to find any previous discussion of the significant overestimate of radiation transport that comes from using Voigt profiles without pedestals, nor

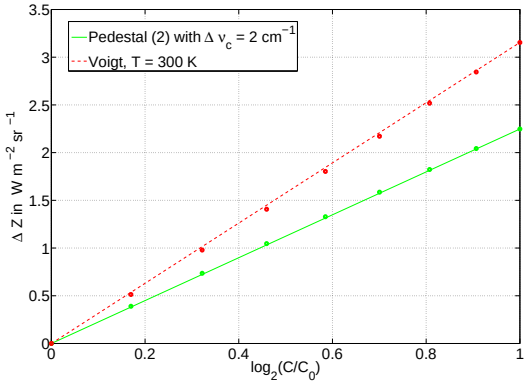


FIG. 1. (Color online) Line-by-line (points) calculation from (24) of clear-sky downwelling increments, $\Delta Z$, versus $\ln(C/C_0)$ for $C_0 = 400$ ppm of $CO_2$. The Arrhenius approximations (lines) of (3), have the parameters (in W $m^{-2}$ $sr^{-1}$): $Z_2 = 3.15$ for Voigt profiles $Z_2 = 2.25$ for lines with pedestals.

have we been able to determine what assumptions about far-wing lineshapes were used in the models discussed by Fyfe et al. [1]. Comparable or larger effects should occur for the radiation transport at the tropopause [7], where "radiative forcing" of global warming is commonly calculated. Harde, in a private communication, confirms that his recent model [8], one of the few that predicts warming comparable to observations, used Voigt profiles without pedestals. Experiments summarized in Fig. VII.15 of reference [3], show that models with Voigt lineshapes predict far more thermal emission at the edges of the 667 $cm^{-1}$ $CO_2$ band than is actually observed.

We hope this introduction makes clear that it is important to eliminate uncertainties due to far-wing lineshapes. Next we outline the physics of pedestals, and we conclude by suggesting experiments to characterize $CO_2$ pedestals accurately enough to eliminate this source of uncertainty in climate models. In cloud-free air, radiation transport is governed by the Schwarzschild equation [9]

$$\cos\theta \frac{\partial I}{\partial z} = \kappa(B - I). \tag{4}$$

Here $I = I(\nu, z, \theta)$ is the brightness of a pencil of radiation of spatial frequency $\nu$ (in cycles/cm or $cm^{-1}$) at the altitude $z$. The pencil makes an angle $\theta$ to the vertical. The local thermal emission of the atmospheric molecules is proportional to the product of the attenuation coefficient $\kappa = \kappa(\nu, z)$ and the local Planck brightness

$$B = \frac{2hc^2\nu^3}{e^x - 1}, \tag{5}$$

The ratio of the photon energy to the thermal energy is $x = hc\nu/k_BT$; $k_B$ is Boltzmann's constant and $T = T(z)$ is the temperature of the atmosphere. The contribution of $CO_2$ molecules to the attenuation coefficient $\kappa$ is

$$\kappa = CN \sum_{ul} \sigma_{ul}. \tag{6}$$

where $N = N(z)$ is the molecular number density of dry air. We assume that the $CO_2$ molecules are uniformly mixed so $C$ is independent of altitude. The contribution of the transition $l \to u$ to the absorption cross section is

$$\sigma_{ul} = S_{ul} G_{ul}. \tag{7}$$

The frequency-independent line strength is

$$S_{ul} = \pi r_e f_{lu} \left(1 - e^{-x_{ul}}\right) \eta_{ul} W_l / Q. \tag{8}$$

The isotopomer fractions are $\eta_{ul} = 0.9843$ for $^{16}O^{12}C^{16}O$, $\eta_{ul} = 0.0110$ for $^{16}O^{13}C^{16}O$, *etc.*. The classical electron radius is $r_e = 2.82 \times 10^{-13}$ cm, the oscillator strength of the absorption line is $f_{lu}$, the unnormalized probability to find the isotopomer in the lower state is $W_l = e^{-E_l/k_BT} g_l(2j_l + 1)$, where $j_l$ is the rotational quantum number of the lower level, and the coefficient $g_l$ (often 1 or 0) depends on whether two oxygen isotopes are identical. The partition function is $Q = \sum_l W_l$. The ratio of the resonant photon energy to the thermal energy is $x_{ul} = hc\nu_{ul}/k_BT$, and the factor $e^{-x_{ul}}$ in (8) accounts for stimulated emission on the transition $u \to l$. Numerical values for $S_{uv}$ for many thousands of transitions of $CO_2$ and other molecules have been measured and tabulated [2].

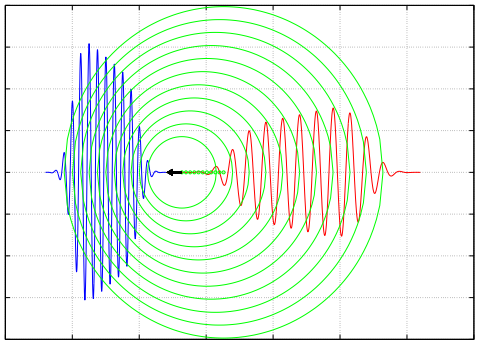

FIG. 2. (Color online) Snapshot (with exaggerated parameters) of red-shifted electric fields $E$ of radiation emitted in a direction antiparallel to the velocity of an oscillating $CO_2$ molecule, or blue-shifted radiation emitted parallel to the velocity. The molecule is collisionally excited and radiates freely until deexcited by a second collision. The green circles are the loci of peaks of $E$. Doppler shifts, radiative damping and the finite time of free oscillation produce the Voigt-profile core of the resonant line. Radiation during collisional excitation and de-excitation produces the pedestal.

The lineshape function $G_{ul}(\nu)$ of (7) is proportional to the spectral power density of the molecular radiation, or

$$G_{ul}(\nu) \propto |\tilde{E}(\omega)|^2 \propto \omega^4 |\tilde{D}(\omega)|^2, \tag{9}$$

with the normalization condition $\int G_{ul} d\nu = 1$. The spatial frequency $\nu$ and radian frequency $\omega$ are related by $\omega = 2\pi c\nu$. The Fourier transform of the observed electric-field is $\tilde{E}(\omega) = \int dt\, E(t) e^{i\omega t}$, and the Fourier transform of the molecular dipole moment $D(t)$ that launched the field is $\tilde{D}(\omega) = \int dt\, D(t) e^{i\omega t}$. Fig. 2 shows the electric fields radiated by a $CO_2$ molecule that is collisionally excited at time $t = 0$ and deexcited by a second collision at time $t = \tau$. From inspection of Fig. 2 and (9) we see that the lineshape functions of (1) have much the same physics as atomic-clock lineshapes [10], where Cs atoms from an atomic beam are excited by an oscillatory magnetic field of a first Rabi loop, analogous to the excitation collision of Fig. 2. After a period of free oscillation in flight, they are deexcited by a second Rabi loop, analogous to the deexcitation collision of Fig. 2.

The dipole moment associated with the transition from

$u$ to $l$ evolves as

$$\ddot{D} = -\omega_{ul}^2 D + \frac{\gamma_{ul}}{\omega_{ul}^2}\dddot{D} + \omega_{ul}^2 \tilde{\alpha}_0 F. \quad (10)$$

Most of (10) comes from a solution of Schroedinger's equation for a molecule driven by a real, classical electric field $F$, for example, the quadrupole field a colliding $N_2$ molecule. The term proportional to $\dddot{D}$ is the Abraham-Lorentz radiation damping [11], and $\gamma_{ul}$ is the spontaneous decay rate from $u$ to $l$. The Bohr frequency is $\omega_{ul} = 2\pi c\nu_{ul} \approx 10^{14}$ s$^{-1}$ The contribution of virtual transitions $l \to u$ to the static polarizability is $\tilde{\alpha}_0 = c^2 S_{ul}/(\pi\omega_{ul}^2)$. Taking the Fourier transform of both sides of (10) we find

$$\tilde{D} = \tilde{\alpha}\tilde{F}. \quad (11)$$

where the polarizability at frequency $\omega$ is

$$\tilde{\alpha} = \frac{\omega_{ul}^2 \tilde{\alpha}_0}{\omega_{ul}^2 - \omega^2 - i\gamma_{ul}\omega^3/\omega_{ul}^2}. \quad (12)$$

Transforming (11) to the time domain we find

$$D(t) = \int d\tau\, \alpha(\tau)\, F(t-\tau). \quad (13)$$

For $\tau < 0$, we set $\alpha(\tau) = 0$, thereby neglecting a tiny, non-causal contribution from the pole of $\tilde{\alpha}(\omega)$ at $\omega_0 \approx i\omega_{ul}^2/\gamma_{ul}$. For $\tau \geq 0$ the response function is very nearly

$$\alpha(\tau) = \int \frac{d\omega\, \tilde{\alpha}(\omega) e^{-i\omega\tau}}{2\pi} = \omega_{ul}\tilde{\alpha}_0 e^{-\gamma_{ul}\tau/2} \sin\omega_{ul}\tau. \quad (14)$$

Consider an impulsive field

$$F_k = \hat{F}_k + \hat{F}_k^* \quad \text{with} \quad \hat{F}_k = A(t-t_k)e^{i\phi_k - i\omega_c t}. \quad (15)$$

The envelope $A(t-t_k)$ is negligibly small if $|t-t_k| \geq \tau_c$, where $\tau_c \approx 10^{-12}$ s is a characteristic impulse duration, and $\phi_k$ is an arbitrary complex number. The characteristic frequency of the pulse, $\omega_c \approx \omega_{ul}$, can be thought of as the near-resonant vibration-rotation frequency of a colliding molecule, for example $N_2$ or $O_2$, that exchanges energy with the $CO_2$ molecule. According to (13) and (14), for times $t > t_k + \tau_c$, the dipole moment induced by $F_k$ is $D_k = \hat{D}_k + \hat{D}_k^*$ where

$$\hat{D}_k \sim \frac{i\omega_{ul}\tilde{\alpha}_0 \tilde{A}(\omega_+ - \omega_c)}{2} e^{i\phi_k + i(\omega_+ - \omega_c)t_k - i\omega_+ t}. \quad (16)$$

Here $\omega_+ = \omega_{ul} - i\gamma_{ul}/2$, and $\tilde{A}(\omega) = \int dt\, A(t)e^{i\omega t}$. According to (16), the molecule will "ring" at the Bohr frequency $\omega_{ul}$ for a time of order $\gamma_{ul}^{-1} \approx 1$ s [12] after the end of the impulse.

Let the molecule be excited by an initial collision at time $t_1 = 0$ and oscillate freely until it loses its oscillation energy in a second collision at the time $t_2 = \tau$, as sketched in Fig. 2. This can be described by the bipulse field $F_\tau = \hat{F}_\tau + \hat{F}_\tau^*$, where

$$\hat{F}_\tau = A(t)e^{-i\omega_c t} - A(t-\tau)e^{i(\omega_c - \omega_+)\tau - i\omega_c t}. \quad (17)$$

One can use (16) to verify that the ringing of the second pulse of (17) cancels that of the first. For $\omega > 0$, the Fourier transform of (17) is

$$\tilde{F}_\tau(\omega) = \tilde{A}(\omega - \omega_c)\left[1 - e^{i(\omega-\omega_+)\tau}\right]. \quad (18)$$

Substituting (18) into (11) and using the one-pole approximation to the polarizability, $\tilde{\alpha} \approx \omega_{ul}\tilde{\alpha}_0/[2(\omega_+ - \omega)]$, for frequencies $\omega \approx \omega_{ul}$ we find

$$\tilde{D}_\tau(\omega) \propto \tilde{A}(\omega - \omega_c)\frac{1 - e^{-i(\omega_+ - \omega)\tau}}{\omega_+ - \omega}. \quad (19)$$

In the atmosphere, the probability to find the value of $\tau$ between $\tau$ and $\tau + d\tau$ is $e^{-\Gamma_{ul}\tau}\Gamma_{ul}d\tau$, where $1/\Gamma_{ul}$ is the mean time of free oscillation between collisions . Averaging (9) over this distribution gives

$$G_{ul}(\nu) \propto \omega^4 \int_0^\infty d\tau\, \Gamma_{ul} e^{-\Gamma_{ul}\tau} |\tilde{D}_\tau(\omega)|^2. \quad (20)$$

Evaluating the integral (20) with (19) and normalizing so that $\int G_{ul} d\nu = 1$, we find (1), where the pedestal function is

$$\chi_{ul}(\nu) = \frac{|\tilde{A}(\omega - \omega_c)|^2}{|\tilde{A}(\omega_{ul} - \omega_c)|^2}. \quad (21)$$

The half-width at half maximum, $\mu_{ul}$, of the Lorentzian line core of (1) is

$$\mu_{ul} = \frac{\Gamma_{ul} + \gamma_{ul}/2}{2\pi c}. \quad (22)$$

The placeholder pedestal (2) would be produced by the envelope $A(t) = A_0\ \mathrm{sech}(t/\tau_c)$, with collision duration $\tau_c = 1/(\pi^2 c\Delta\nu_c)$ and a resonant frequency $\omega_c = \omega_{ul}$.

The minimalist theoretical discussion above can be generalized to sequences of collisions that do not completely destroy the oscillating dipole but introduce amplitude or phase shifts and transfer excitation between different Bohr frequencies (line mixing). For the relatively hard collisions that interrupt the free oscillations of $CO_2$ molecules, the basic form (1) of the lineshape function remains: a Lorentzian/Voigt core multiplied by a pedestal that represents molecular radiation emitted during finite-duration collisions.

We conclude with a brief discussion of experimental determinations of far-wing line shapes. Modern instrumentation [13] could greatly improve on Langley's pioneering experiments [14] on the attenuation of infrared moonlight, used by Arrhenius [15] in the first attempts

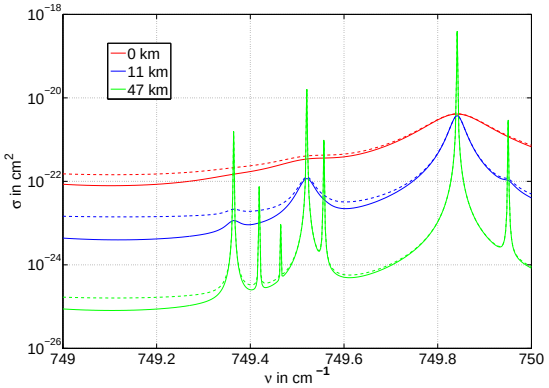


FIG. 3. (Color online) Cross sections $\sigma_{ul}$ of (7) in the high-frequency wing of the 667 cm$^{-1}$ absorption band of $CO_2$. The solid lines have pedestals (2), with a width of $\Delta\nu_c = 2$ cm$^{-1}$, corresponding to an envelope with a duration $\tau_c = 1.69$ ps. The dashed lines are from Voigt profiles without pedestals. The resonance lines come from P and R transitions out of excited vibrational states of the most abundant isotopomer, $^{16}O^{12}C^{16}O$, except for the rightmost line at $\nu_{ul} = 749.951$ cm$^{-1}$, an R line for absorption from the first excited vibrational state of the isotopomer, $^{16}O^{13}C^{16}O$. The temperatures in K at the sample altitudes 0, 11 and 47 km are 296, 224.5 and 278.5. The pressures in Torr are 760, 178 and 1.

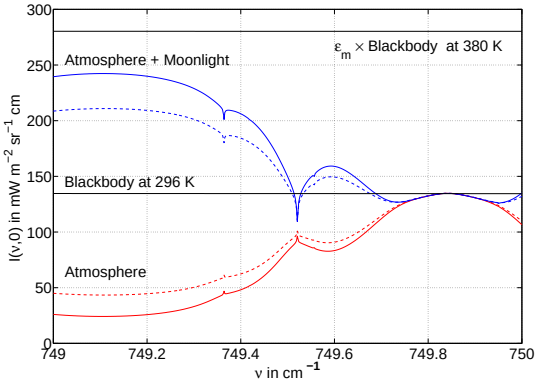


FIG. 4. (Color online) Zenith downwelling, $I(\nu, 0, \pi)$, from (23) for the conditions of Fig. 3. The solid lines come from profiles with pedestals (2) of width $\Delta\nu_c = 2$ cm$^{-1}$ . The dashed lines come from Voigt profiles without pedestals.

to estimate warming from additional $CO_2$ in the atmosphere. A particularly useful spectral region is the high-frequency edge of the 667 cm$^{-1}$ band, where there there is little interference from lines of water vapor. $CO_2$ absorption cross sections (7) in the representative interval $749 - 750$ cm$^{-1}$ are shown in Fig. 3. For a ground-based instrument recording the apparent brightness of the center of the full moon at the zenith, the solution of (4) with $\theta = \pi$ is

$$I(\nu, 0, \pi) = \int_0^\infty B(z) e^{-\rho(z)} \kappa dz + \epsilon_m B_m \, e^{-\rho(\infty)}, \quad (23)$$

where $B_m$ is the brightness of the moon at a representative temperature of $T_m = 380$ K and a representative thermal emissivity of $\epsilon_m = 0.9$. The optical depth from the surface to altitude $z$ is $\rho(z) = \int_0^z \kappa(\nu, z')dz'$. Shown in Fig. 1 are increases, $\Delta Z$, of the clear-sky, zenith downwelling, $Z$, integrated over the entire 667 cm$^{-1}$ frequency band

$$Z = \int_0^\infty I(\nu, 0, \pi) d\nu, \quad (24)$$

due to increases of $CO_2$ concentrations $C$ above the present level of $C_0 = 400$ ppm.

Representative downwelling spectra (23) from the moon and the atmosphere or from the atmosphere alone with $B_m = 0$ are shown in Fig. 4. Near the strong resonance at 749.842 cm$^{-1}$ the downwelling is close the Planck brightness (5) at the earth's surface temperature. There most of the downwelling comes from the first few hundred meters of the atmosphere, which is only slightly cooler than the surface. The small, extremely narrow resonances are from molecules in the upper stratosphere, where linewidths are close to the Doppler limit of about 0.0006 cm$^{-1}$ $\approx$ 20 MHz.

As one can see from Fig. 4, far wings have the largest effect for frequencies in the gaps between unsaturated $CO_2$ lines near the band edges. Because the surface downwelling (or the analogous radiative forcing at the tropopause) involve emission and absorption over a large range of temperatures and pressures, measurements with high spectral resolution in the open atmosphere, at various zenith angles, and comparison of these measurements with model predictions like that of Fig. 4 would allow one to experimentally determine far-wing broadening parameters (pedestal functions) for accurate modelling of radiation transfer.

This work received no outside funding. We are grateful to colleagues who have reviewed early drafts of this paper and made many helpful suggestions.

[1] J. C. Fyfe, N. P. Gillett, F. W. Zwiers, Nature Climate Change **3**, 767 (2013)
[2] L. S. Rothman et al., JQSRT **110**, 533 (2009)
[3] J-M. Hartmann, C. Boulet and D. Robert, *Collisional Effects on Molecular Spectroscopy* (Elsevier, Amsterdam, 2008)
[4] Q. Ma, R. H. Tipping, C. Boulet and J-P. Bouanich, Applied Optics **38**, 599 (1999)
[5] D. P. Edwards, L, L. Strow, J. Geophys. Res. **96**, 20,859 (1991)
[6] D. J. Wilson, J. Gea-Banacloche, Am. J. Phys. **80**, 306 (2012)
[7] G. Myhre, E. J. Highwood, K. P. Shine Geophys. Res. Letters **25**, 2715 (1998)
[8] H. Harde, Open Jour. Atmos. and Climate Change;

ISSN(Print): 2374-3794 ISSN(Online): 2374-3808 DOI: 10.15764/ACC.2014.03001
[9] S. Chandrasekhar, *Radiative Transfer* (Dover, New York, 1960)
[10] J.H. Shirley, W. D. Lee, G. D. Rovera, R. E. Drullinger, IEEE. Trans. Instr. Meas. **44**, 136 (1995)
[11] S. Jackson, *Classical Electrodynamics (Second Edition)* (Wiley, New York, 1975)
[12] H. Statz, C. L. Tang, G. F. Koster, J. Appl. Phys. **37**, 4278 (1966)
[13] D. D. Turner et al. Geophys. Res. Letts. **39**, L10801 (2012)
[14] S. P Langley, *Researches on Solar Heat and its Absorption by the Earth's Atmosphere* (Government Printing Office, Washington, 1884)
[15] S. Arrhenius, London, Edinburgh and Dublin Philosophical Magazine and Journal of Science **41**, 237 (1896)